THE EFFECT OF WATER MOLECULES ON HEADGROUP ORIENTATION AND SELF-ASSEMBLY PROPERTIES OF NON-COVALENTLY TEMPLATED PHOSPHOLIPIDS.

A Thesis

Submitted to the Faculty

of

Purdue University

by

John A. Biechele-Speziale

In partial Fulfillment of the

Requirements for the Degree

of

Master of Science

May 2019

Purdue University

West Lafayette, Indiana

THE PURDUE UNIVERSITY GRADUATE SCHOOL
STATEMENT OF THESIS APPROVAL

Dr. Shelley Claridge, Chair

     Department of Chemistry

Dr. Scott McLuckey

     Department of Chemistry

Dr. Chittaranjan Das

     Department of Chemistry

Approved by:

     Dr. Christine Hrycyna

          Head of the Department Graduate Program

ACKNOWLEDGEMENTS

I am grateful to my family, Jen, Sherri, and Dana, for listening to my incessant ranting when the instruments were down in lab. Thank you for your support and your troubleshooting ideas when I couldn't see straight.

I am immensely thankful for the opportunities and mentoring provided by Dr. Eric Conte, Dr. Stuart Burris, Dr. Shing-Yi Suen, and Dr.Yong-Ill Lee in my undergraduate career, without these experiences I don't know if I could have made it through my program as far as I did with any sense of which way is up.

A huge thank you also goes out to the Gatton Academy, specifically Tim Gott and the Ziegler/Ernst tag-team duo, and the crucible they put me through that continues to shape my thinking and problem solving. It refined me into a person who always wants to surpass his best.

I am grateful to Professors Wirth and Claridge, who have both graciously put up with me and helped me decide how to change paths to something I would find more fulfilling.

Finally, I am so grateful to my beautiful wife Jenny, who not only has looks, but brains, patience to the moon and back, and a kind heart to back it all up. Her support and patience has kept me on track even when I felt I was to fall off.

TABLE OF CONTENTS

LIST OF FIGURES

ABSTRACT

Biechele-Speziale, John A., Purdue University, May 2019. The Effect of Water Molecules on Headgroup Orientation And Self-Assembly Properties of Non-Covalently Templated Phospholipids. Major Professor: Shelley A. Claridge

Simulations of various hydration levels of lamellar phase 23:2 Diyne PC were performed, and subsequent, serial docking simulations of a tyrosine monomer were replicated for each system in both hydrated and dehydrated states. The goal was to evaluate how hydration impacts self-assembly and crystallization on the surface, and whether or not these simulations, when run sequentially, could determine the answer. It was discovered that hydrated and dehydrated surfaces behave differently, and that headgroup orientation plays a role in the initial docking and self-assembly process of the tyrosine monomer. It was also determined that potential energy as a sole metric for determining whether or not a specific conformation of intermolecular orientation is not entirely useful, and docking scores are likely useful metrics in discriminating between conformations with identical potential energy values.

CHAPTER 1: INTRODUCTION

1.1 The limitations of current technology.

The transistor, invented originally in 1925, and improved to the point of use in 1947 and 1954, began as a relatively large device capable of amplifying and switching electrical signals, and are now the basis of integrated circuits present in devices worldwide.[1] Produced at a junction between P and N type silicon, the transistors of today are significantly smaller than their previous counterparts. In fact, they are at the length scale of approximately 7nm.[2] However, continuing to decrease the size of these components any further presents interesting challenges, primarily involving the quantum tunneling effects in the material, which inhibits their ability to act as switches. This occurs as the electrons are capable of tunneling through the gate oxide layer, which prevents the storage of charge necessary for these components to be useful as switches that comprise logic gates.[3] Additionally, fabricating complex structures at such the nanoscale is difficult in general. Self-assembly, specifically in soft materials, has been proven possible in graphene FETs; but this technology is very recent, and more work is necessary to actualize devices made of such materials.[4] This lower bound on size presents a limitation that, if surpassed, could further increase the density of integrated circuits and thus, computational efficiency.

Yet another dependency of devices that utilize integrated circuits is electricity. Despite our abilities to run more complex computations on diminishing amounts of power, in phones for example, modern scientific quandaries require continually increasing amounts of storage space, RAM, and electricity, as well as more complex architecture and programming. Considering the amount of power consumed to facilitate the operation of these machines, an even more costly issue to address is that of heat dissipation. As the number of transistors on a chip increases, and the heat produced from the circuits does as well, and to cool these components, even more heat is produced/energy is utilized by the heat-pumps, fans, and radiators. Additional heat is also generated to produce the electricity to power the systems, particularly through non-renewable fuels. Even worse, heat dissipation is becoming more of an issue as climate change continues, due to the heat we are producing both in running our many machines, and keeping them cool enough for use. While the immediate effects of heat production are nearly unnoticeable, over time and with millions of users, the heat being produced by these devices is quite large. In fact, new meta-materials have been developed to help cool densely populated areas, as the heat produced just from air conditioning was increasing the local temperature drastically.[?] As global carbon

dioxide levels continue to rise, it may be worth while looking into producing more sustainable sources of electricity, such as solar, to power these immensely useful and nearly ubiquitous machines, and the reduce the carbon related impact on our planet in the process.

Current solar cells operate at an average efficiency of 37% (with a recent record of 45%), and by increasing their efficacy, more energy could be generated with less material; thus, production costs could be reduced.[5] The mechanism by which solar cells function is through generating electron-hole pairs in either boron/phosphorous doped semiconductors, or organic thin-films. Specifically, the exciton pair is generated in the p-type material, which then must diffuse to the n-type material for the charge separation to take place, and electric potential to be generated. However, the distance between this pair, and between the hetero-junction between the p and n type materials is often too large to guarantee the charge separation of the exciton. When this process fails, typically when the distance from the exciton to the heterojunction is greater than 10nm, the electron and hole recombine, and no current is produced.[6,7] At the moment, the amorphous, unordered nature of the materials, specifically in organic films, is one of the main limiting factors in the efficiency of organic photovoltaics. By reducing the size of these materials, thus decreasing the distance between the exciton and the hetero-junction, it should be possible to significantly increase their efficiency. This, in turn, allows more energy to be produced, at a reduced environmental and economical cost.

1.2 The questions

As the discovery of more efficient photovoltaic and electronic technologies are necessary for the development of sustainable electricity, we must ask: is it possible to move past this size limitation and produce smaller and more efficient devices? And if so, can it be done with readily abundant materials that are easier to fabricate than doped silicon, and simpler to structure than amorphous thin films? Additionally, could the manufacturing process be primarily additive in nature, rather than subtractive, to increase the efficiency of material consumption and reduce the burden of recycling the waste produced during manufacturing?

The goals of my lab lies in answering these questions, and the primary focus of our work is the production of nanoscale electronics and photovoltaics out of bio-inspired, environmentally-friendly materials, which are non-covalently bound to graphene in a striped, or lamellar, phase, with a sitting orientation.[8,9] Considering that lipids in cell membranes are regularly responsible for orienting various proteins and components within the membrane, it may be possible to spatially orient other nanostructures with high fidelity that are resilient to the addition of other compounds, or other processing steps. Thus far, the lab has been quite successful in demonstrating the ability of these

monolayers to effectively template, or epitaxially orient, certain nano-structures that deposit onto them.[10,11] A key example towards the generation of nano-circuitry was developed by Ashlin Porter, who has succeeded in templating gold nanowires onto these surfaces, and Anni Shi, who is currently experimenting with orienting cadmium sulfide nanorods.

The benefit of the lamellar phase over other orientations is the relative thickness of the monolayer decreases from the length of the molecule, which stands end to end on the surface, to roughly half a nanometer, the thickness of the molecule.[12–15] This reduction in size should allow for the better transfer of electrons from attached monolayers to the highly conductive graphene sub-structure, which provides a regular geometry onto which the alkyl chains of various molecules can be aligned in a highly ordered state, and over relatively long length scales.[16] Yet another benefit of these lamellar phases, is the precise control over the distance between hydrophobic/hydrophilic moieties (controlled by the length of the molecule), which, allows for control over where different molecules may adsorb to the surface.[17]

While the deposition of diynoic acids is fairly well understood at this point,[12,18] the use of lipids to layer additional monolayers on top of the graphene-bound lamellar phases, and producing specific structures with epitaxial matching to these pre-existing templates can be challenging. There is a wealth of information on the assembly of micro-crystals and nanostructures on standing phase monolayers; however, the orthogonal functionalities on sitting phases may influence crystallization and assembly differently.[11,19–24] Thus, the primary focus of my work has been to determine how the interactions of these headgroups with varying humidity environments would effect the orientation of these lipids, specifically the hydrophilic headgroups, and how this change in orientation may effect the ability of different desirable materials, such as nano-wires or nano-crystals, to adhere or form on the monolayer in this altered environment.

1.3 The Selection of Graphene as a foundation.

Graphene was selected as the substrate onto which a majority of the materials of interest were templated onto (although Molybdenum Disulfide has also been used). Graphene was chosen for a number of reasons, which are inherent to its structure and interesting properties. Primarily, it is a highly conductive monolayer of crystalline carbon which forms a hexagonal lattice. The conducting properties of this material cannot be overstated. The ability for charge to propagate through it is quite high, and has demonstrated superconductor capabilities when aligned in a particular way.[25] Additionally, the highly ordered crystalline structure has a length scale of approximately 2.46, and the typical length for alkyl chains is 2.56. The epitaxial mismatch is very low between these values, which lends itself to high epitaxial alignment that

allows for ordering of alkyl chains on graphene in a predictable fashion.[18] The structure of graphene, as well as the epitaxial mismatch between the graphene lattice and the layered phases that template onto it is shown in Figure 1.
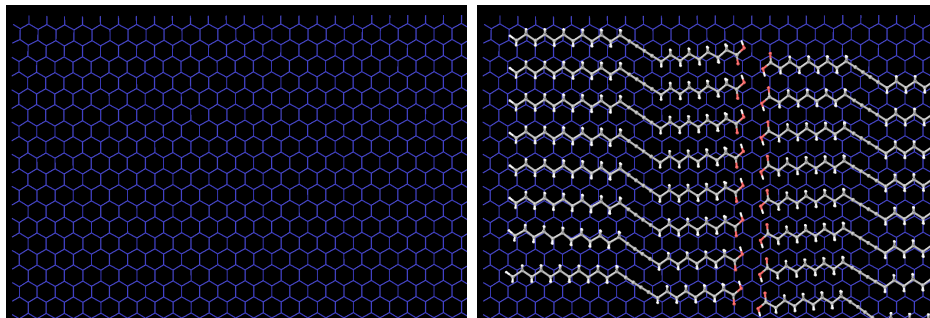

Figure 1: Graphene lattice, illustrating the hexagonal arrangement of carbon, and the alignment of Pentacosadiynoic acid (PCDA) on the surface. The mismatch between the acid and the lattice is noticeable near the hydrocarbon tails, where there is imperfect alignment.

However, in most instances, highly ordered pyrolytic graphite (HOPG) is used as a graphene analogue, considering it is more robust, cleavable to produce fresh surfaces, and does not have the confounding issue of graphene being so thin, that the surface it is prepared on can be "visible" to the monolayers that are deposited onto the graphene. This isolation from other materials allows the HOPG to function similarly to an idealized version of graphene; however, it forgoes its incredibly conducting properties, particularly in the z-axis (between graphene sheets), for increased stability and re-usability.

1.4 The Epitaxial Alignment of Lipids on Graphene via Langmuir-Schaefer Conversion.

The epitaxial mismatch between alkyl chains and the graphene lattice is what lends to the high degree of ordering of deposited materials. This can be clearly seen in diynoic acids, specifically PCDA, which exhibits excellent ordering and yields highly reproducible lying down structures.[12,18,26] To produce these monolayers, Langmuir-Schaefer deposition is utilized. While the process of lying phase deposition is fairly well understood, especially for PCDA, producing sitting phase instead of standing or laying phase monolayers requires some experimentation to determine at which point along the adsorption isotherm the lipids are compressed enough to self-assemble, but not compressed to the point of standing phase transfer.[17] Additional parameters including the concentration of the solution used to produce the film, as well as the temperatures of both the liquid subphase, and the solid substrate can be controlled to generate certain effects.[16]

Despite the high ordering of the diynoic acids, the head groups of these molecules are typically hydrogen bound to each other and are oriented directly against the graphene sheet; thus, they are not accessible to the solution phase after they are bound to the surface.[27] However, another set of molecules has been identified: phospholipids. They align in a manner similar to that of the diynoic acids but, have a flexible, dual charged head group, with an ethyl bridge separating the charge. The flexibility granted by the ethyl bridge, and the high electron density of the phosphate group, which can be stabilized by the highly conjugated graphene substructure, allows for the production of lamellar sitting phases, rather than laying phases, with head group sections, specifically the terminus, that are accessible to the bulk solution for chemistry, similar to the effects of lysine snorkeling found in transmembrane helices.[14,15] This can be seen in Figure 2.

An additional useful characteristic of the lipids, is that they can contain a diyne moiety at some point within the carbon tail. When exposed to ultraviolet light, these diynes will form an ene-yne alternating molecular wire which can transfer charge efficiently across the length of the now polymerized lipids.[28] Even better, this polymerization step improves the stability of the lipid layer to solvent processing, and allows for transfer of other materials from bulk solution without heavily disrupting the underlying lamellar structure.[16]

The change from tightly bound headgroups to those that are bulk accessible allows for orthogonal ordering of polarity at both the hydrophobic tails, which are in strong epitaxy with the graphene lattice, and with the terminal moiety which retain their typical properties such as $pK_{\frac{1}{2}}$, which is not seen in the diynoic acids, or the nonterminal moiety of the head group.[27]
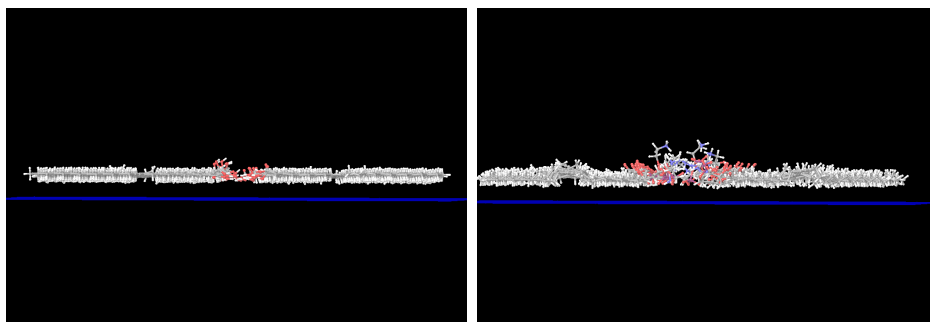

Figure 2: Illustration of the difference between lying phase (left) and sitting phase (right). The lying phase lies nearly parallel to the graphene surface, where as the sitting phase has the headgroup raised above the graphene and is accessible to the solvent.

1.5 Effects of Headgroup Orientation

As mentioned, the pK$_\frac{1}{2}$ of the terminal moiety of the lipid aligned on the graphene is identical to that of a lipid in bulk solution; however, this is not the case for other functionalities that are adjacent to the graphene.[27] Due to this effect, the orientation and position of the head-group moieties directly contributes to the ability of the headgroups of the lipids to template molecules above them, and influence their orientation as they either deposit, or nucleate and extend. This is clearly seen in the work with gold nano-wires, as they orient themselves along the lipid rows, despite forming in the bulk solution. The other question is whether or not the lipid rows can properly orient other molecules as they grow on the surface, without prior anisotropic growth. The goal of my research thus far has been to identify whether or not the headgroups of these lipids, specifically diyne PC, are controlled by external factors (such as humidity), and whether or not this control will affect the ability of the lipids to template differing nano-structures. Primarily I have investigated this through the use of simulations, although Ashlin Porter has demonstrated this effect experimentally with her gold wires.

CHAPTER 2: METHODS

2.1 Key Pieces of Information

To determine the effect of hydration level on the orientation of the head groups, the initial step was to place a set amount of explicit water molecules on the graphene bound lipids. The waters were placed in a grid array, centered around the headgroups, and were minimized, and then dynamics were run in a non-solvated system, where the conditions of a surface exposed to humidified air, but not in liquid. This methodology was used to visualize how the explicit waters attached to and influenced the structure of the headgroups. If the simulation was performed in implicit solvent, the waters would be liberated over time and did not adhere appropriately to the head groups.
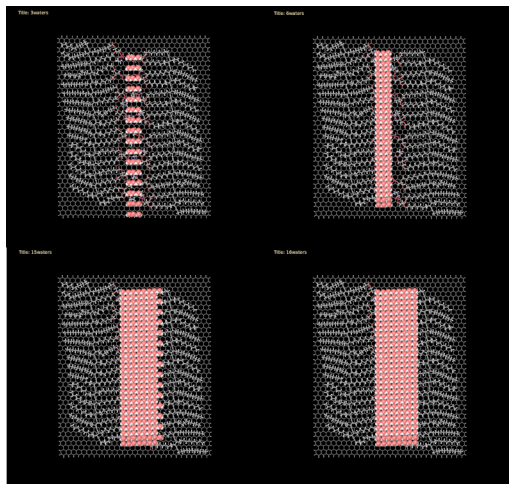

Figure 3: Various examples of initial water orientations, 3,6,15, and 16 waters are shown, 1:16 were actually performed.

The other key question is this: what are reasonable figures of merit (FOM) that can be used to classify the headgroup orientation? In other words, can we reduce the dimensionality of this system to something more simplified, that can be observed to change cleanly, as the number of waters increases? A few reasonable FOMs could include the elevation angle of the head group, as measured from the atom closest to the surface to the one furthest. However, by selecting specifically the charged oxygen on the phosphate group, and the charged nitrogen on the quaternary ammonium group, a reasonable approximation of the elevation and simple visualization of the dipole moment on the surface were achieved. An additional measure is the azimuthal

angle, i.e. the angle between the headgroup and the lamellar median. Both of these angles can then be used to reconstruct the headgroup positioning from the FOMs, in a crude way. To improve the ability to back-calculate this information, and to provide more insight into the orientation, these angles were measured for the ethyl bridge between the phosphorus and nitrogen as well.
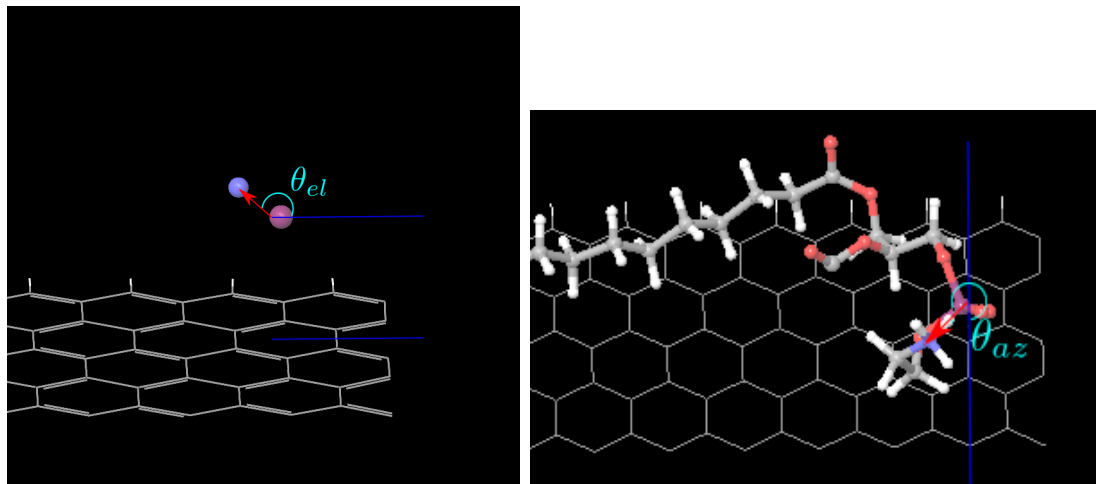

Figure 4: The elevation angle is determined by $90° \pm acos(\frac{N_z - P_z}{\sqrt{(N-P)^2}})$ and the azimuthal angle is determined by $\pm acos(\frac{N_y - P_y}{\sqrt{(N-P)^2}})$. These values are calculated for both the Nitrogen-Phosphorous vector and the Carbon-Carbon vector in the ethyl bridge.

These values were then plotted into a visual representation is to help verify whether patterns existed within the data set or not. To accomplish this, and to determine how the angles of both the head-groups and the ethyl bridges, windrose plots of the angles were made, and then the average values of each set were determined. These centroids were then plotted to determine how the elevation angles were related to the azimuthal angles, and to see if there was any correlation or clustering with the number of water molecules.

2.2 Simulations

For the all the simulations of various systems that were performed, the package Macromodel from Schrödinger was used to run minimizations and dynamics on the various systems, and the front-end Maestro was used to build the systems.[29–31] Macromodel's minimization and dynamics were performed using semi-empirical, rather than ab-initio calculations, in most cases with the OPLS-2005 or OPLSE forcefields. For the docking of the different molecules/dimers onto the lipid surface, the Glide package was used, and scripts were used for batch running and data parsing for all the simulations.

CHAPTER 3: RESULTS AND DISCUSSION

3.1 Hydration Simulations, and Quantifying Differences

After the water structures were generated, they were minimized and dynamics were performed. The simulations were performed in an OPLS-2005 forcefield, without the assumed presence of implicit solvent, to approximate how the headgroups would behave in the presence of limited water, such as in the case of a high humidity environment, but not completely submerged in liquid. This allowed for the discretization of the possible states, which allowed for the dependence of headgroup orientation on relative hydration to be established. The images of minimized waters are shown in Figure 5.

(a) Headgroup images of waters with 1-4 waters per headgroup

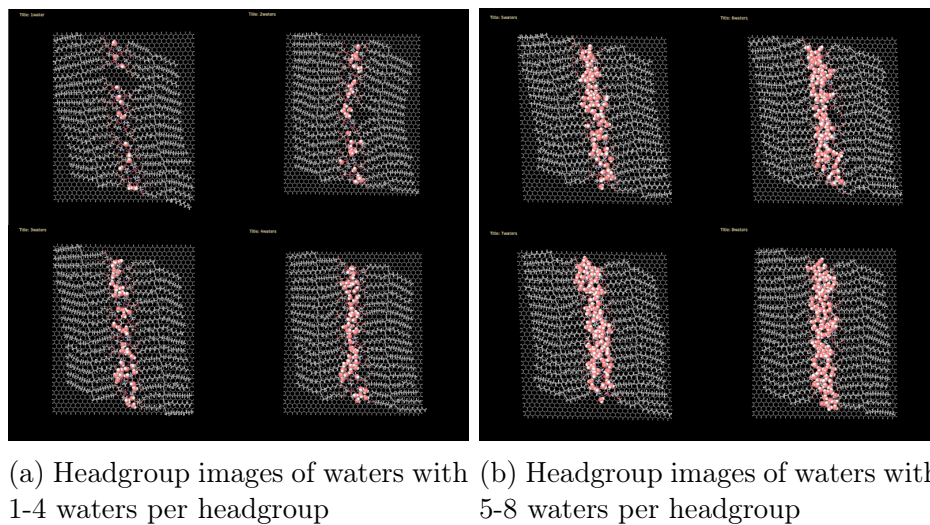(b) Headgroup images of waters with 5-8 waters per headgroup

Figure 5: Headgroup images of waters with 1-8 waters per headgroup, 1-16 were actually performed.

After generating these systems, the systems were reduced to the key figures of merit discussed in the Methods section, specifically the azimuthal and elevation angles of the phosphorous-nitrogen vector, as well as the ethyl bridge between the carbon-carbon vector in the ethyl bridge between the phosphate and the quaternary ammonia. These figures were extracted for each headgroup in each system, and wind-rose plots were produced to aid in visualization.

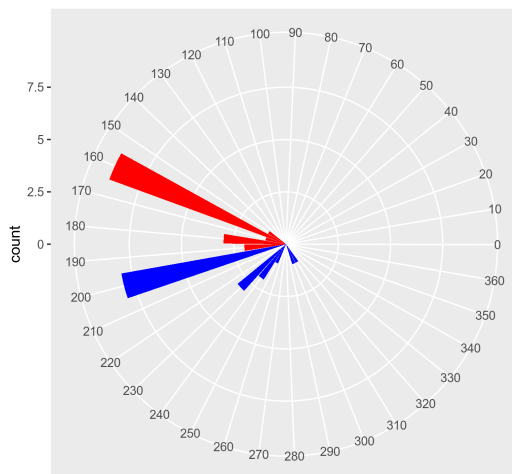## 3.2 Windrose Plots and the Need for an Alternative Visualization.

Figure 6: Example windrose plot, these values for each simulation were determined.

These windrose plots were generated to provide a visualization of a single system's azimuthal and elevation angles for each headgroup (each system contained 16 groups). All the elevation angles for a specific system, as well as the azimuthal angles, were averaged into two values, denoted as either pnaz/pnel or ccaz/ccel. The first two letters indicate whether or not the angle was measured with respect to the phosphorous-amine vector or the carbon-carbon vector in the ethyl bridge between the two charged moieties on the zwitterion. After this data was collected and consolidated for each system, the values were plotted as points, which acted as centroids of the angle distribution, and the phosphorous-nitrogen azimuthal angle was plotted against the ethyl azimuthal angle, to determine if any patterns were present. Interestingly, the data clustered around 4 specific points, and exemplary systems were selected for further simulation.

3.3 Averaging Angle Data for Simpler Visualization and System Selection

For each of the clusters in Figure 7, one example system was selected to represent headgroups with that particular orientation. For the bottom left cluster, the system with 5 waters per headgroup was selected. For the bottom right, 8 waters per headgroup. For the top left, 10 waters per headgroup was selected, and 16 waters per headgroup was selected for the top right. The initial three were selected as examples, but 16 was selected specifically as the theoretical maximum amount of waters that could stay associated with the water head groups in a high-humidity environment.

After these selections were made, the glide package was used to generate the following systems under the premise that subsequent docking of the ligand in question (specifically Tyrosine) could reveal some interesting differences in how initial structural differences in the underlying monolayer may effect the ability of the Tyrosine to crystallize, and that consecutive docking could be a reasonable approximation of how crystallization could take place, ligand by ligand, on the surface.
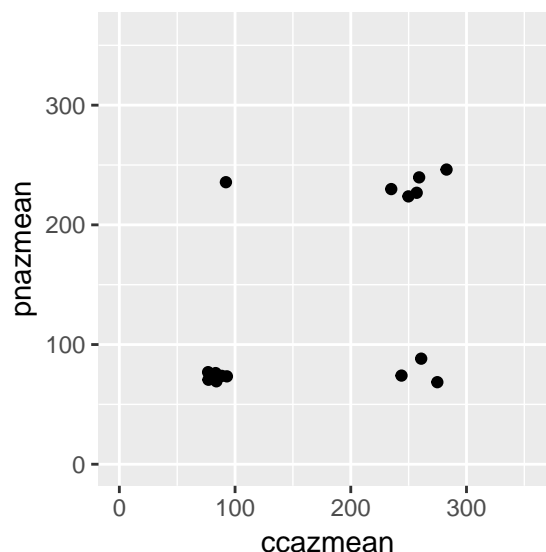

Figure 7: Plot of pn-azimuthal angles vs cc-azimuthal angles, displaying 4 possible conformations. Each point represents and average of 16 head-group positions per system.

3.4 Initial Docking Time-Point Trends

The following systems were generated in two steps with the glide docking protocol, initially with the receptor grid generation prepared to accept peptide based ligands, and then the docking was performed using a single ligand molecule with the previously generated receptor grid. A short bash script looped this system of grid and docking 40 times per system, and 8 total systems were run, one with the waters (denoted as Hydrated) and without the waters (denoted as Dehydrated). Interestingly, after multiple poses were generated, each pose reported the same potential energy, but with different docking scores. This indicates two important features about these simulations: 1. there are multiple possible docking conformations that can be adopted that appear to be equally favorable in terms of potential energy values; 2. the docking score metric may be skewed by what measures are being used to evaluate them. Specifically I rewarded intermolecular hydrogen bonding in terms of the docking score; this seemed reasonable, considering the presence of waters, the aqueous solvent the system would exist in, as well as the hydrogen bond donor and acceptor groups present within the Tyrosine monomer.
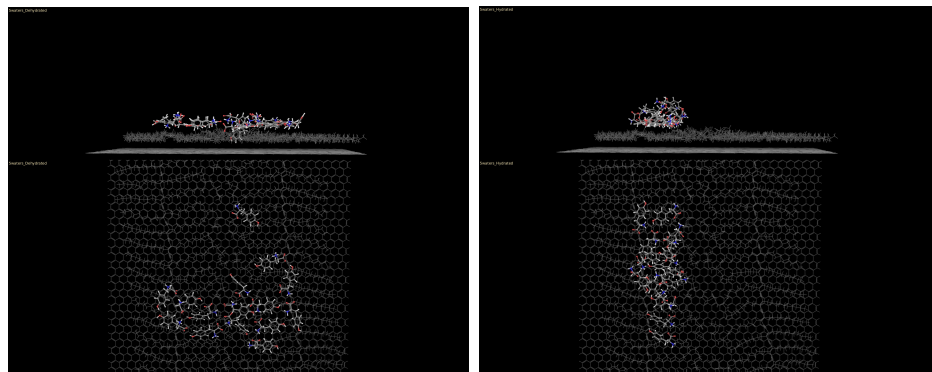
Figure 8: Side and top views of both dehydrated (left) and hydrated (right) models with 5 waters.
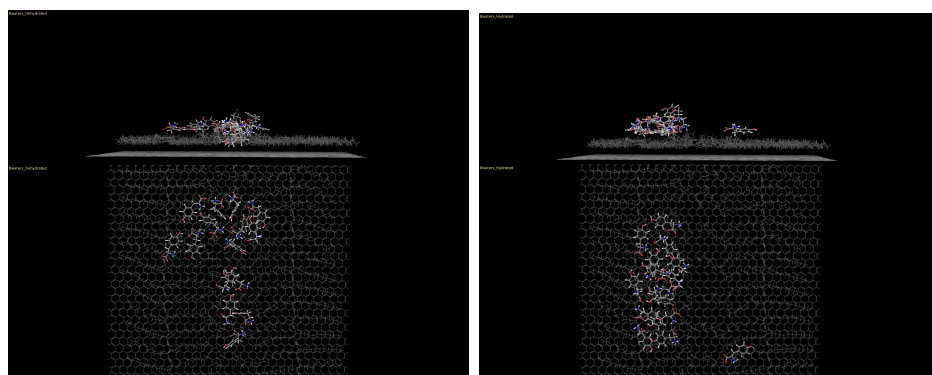

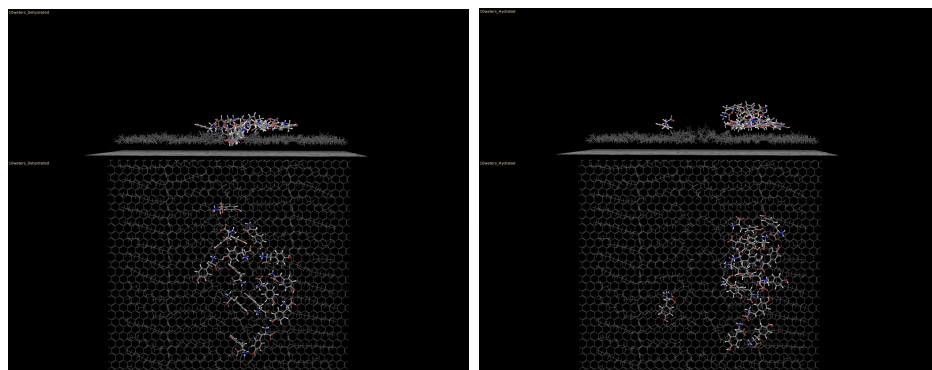Figure 9: Side and top views of both dehydrated (left) and hydrated (right) models with 8 waters.

Figure 10: Side and top views of both dehydrated (left) and hydrated (right) models with 10 waters.
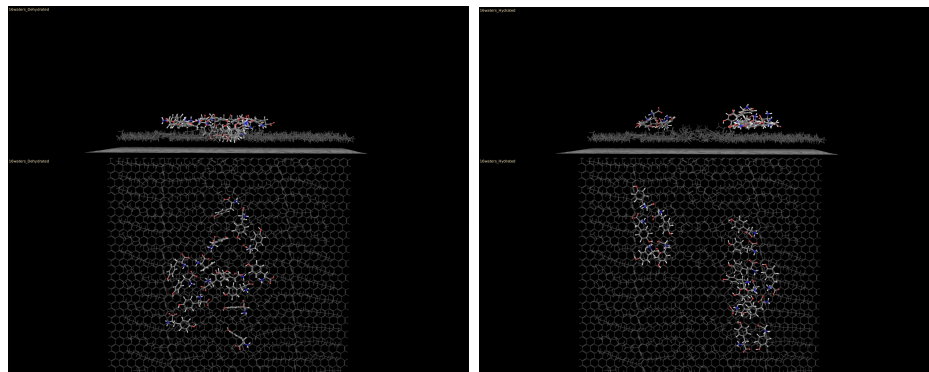
Figure 11: Side and top views of both dehydrated (left) and hydrated (right) models with 16 waters.

Notably, the hydrated models have the water molecules hidden from view to facilitate visualization, but a key characteristic of these models is that the highly polar headgroups are primarily isolated from exposure to the tyrosine monomers in terms of docking, and actively prevent them from entering the gap between the head groups that presents itself after the water molecules are removed from the simulation, as seen most of the dehydrated simulations. Unexpectedly, many of the hydrated simulations appear to assemble asymmetrically along the monomer, with a definitive growth structure on one side of the system, but not on the other. This is later corrected when more monomers were added (all systems were run to at least 32 total monomers), but an early time-point can be predictive of later behavior. The one system that seems to buck the trend is 16, with a definite "handedness", but more balance overall than the other three.

3.5 Late Timepoint Docking Trends

The handedness of the assembly seems to correct itself as the assembly continues; additionally, the gap between the two sections of assembled monomers gradually increases with the number of water molecules on the surface. This makes sense, due to the fact that the water is tightly clustered to the headgroups and prevents the assembly of tyrosine in that space. Another interesting point is the clear amount of disorder on the surface, particularly as the simulations continue. In the initial system, the system seemed fairly consistent with the assembly of the tyrosine monomers in a parallel arrangement to the lipids, to maximize the non-polar interaction between the ring on the monomer and the lipid sheets. This disorder is even more apparent in all of the dehydrated surfaces, specifically due to the fact that the tyrosine prefers to assemble within the gaps between the lipid sheets, if given the chance.
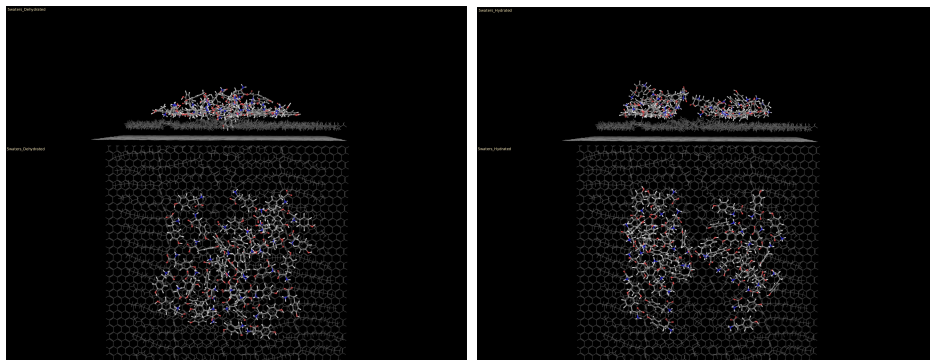
Figure 12: Side and top views of late time point dehydrated (left) and hydrated (right) models with 5 waters.
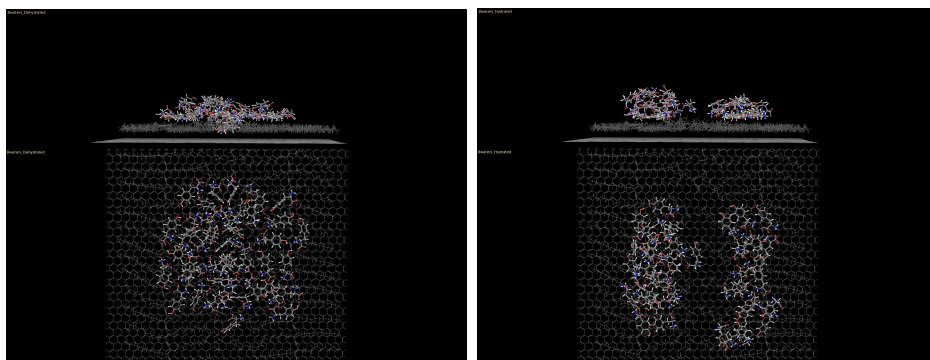

Figure 13: Side and top views of late time point dehydrated (left) and hydrated (right) models with 8 waters.
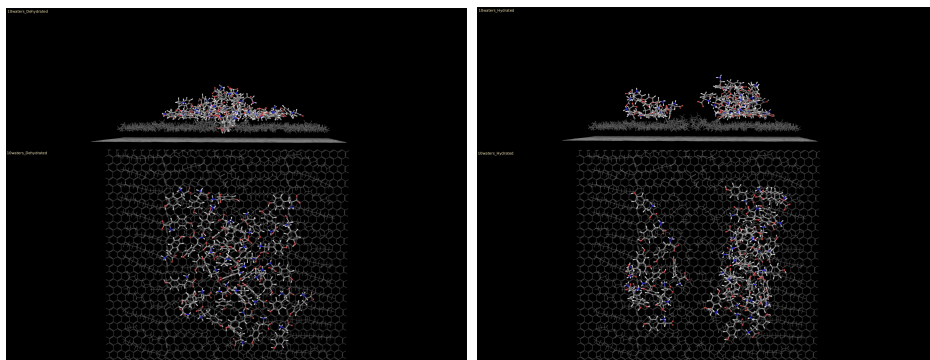

Figure 14: Side and top views of late time point dehydrated (left) and hydrated (right) models with 10 waters.

Considering this is a vastly preferred interaction, but results in a highly disordered system, it is possible that the tyrosine actively displaces water molecules on the
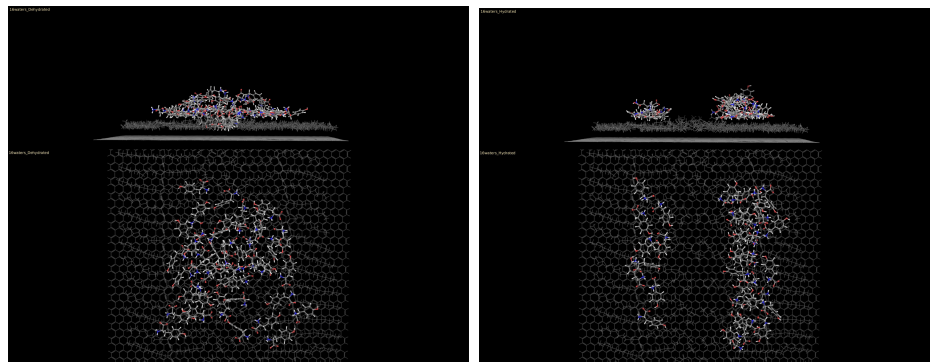
Figure 15: Side and top views of late time point dehydrated (left) and hydrated (right) models with 16 waters.

surface to nestle into these gaps, and produce more disordered surfaces; however, this information could not be readily probed using the current simulation tools that are available, unless further dynamics could be run on the systems for long time steps, and with a way to slowly dehydrate the surface.

Additionally, it should be noted that within certain hydrated systems, there is a preference for the monomer to assemble perpendicular to the surface, with the zwitterion of the amino acid typically facing the zwitterion of the lipid; however, this is a rare interaction, and is only seen to occur after the horizontal assembly of the previously mentioned parallel orientation in a flat sheet-like system. This seems to indicate that there may be some complex, amorphous assembly that is more prone to occurring than direct crystallization.

CHAPTER 4: CONCLUSION

As discussed, there are key differences in the assembly of tyrosine monomers on both hydrated and dehydrated lamellar lipid phases, specifically due to the orientation of the head-groups which also depends on the level of hydration of the head groups to begin with. Thus, a reasonable way to possibly control the various assembly characteristics is to tightly control the ratio of hydration to headgroups. However, doing so may prove difficult in the case of specifically aqueous ligands which are not soluble in mixed media. In this case, other methods should likely be adopted to adjust the suitability of the substrate towards the self assembly of the ligand. Hopefully this information will be useful to progressing future research on crystallization based self-assembly processes on these lipid lamellar phases, which could be further used to produce the environmentally friendly, and energy efficient nanoelectronics and nano-photovoltaics that my lab is striving for.

REFERENCES

[1] November 17 - December 23, 1947: Invention of the First Transistor. https://www.aps.org/publications/apsnews/200011/history.cfm.

[2] IBM Alliance Produces Industry's First 7nm Node Test Chips. undefined, 2015.

[3] Sperling, E. Quantum Effects At 7/5nm And Beyond. 2018.

[4] Li, B.; V. Klekachev, A.; Cantoro, M.; Huyghebaert, C.; Stesmans, A.; Asselberghs, I.; Gendt, S. D.; Feyter, S. D. *Nanoscale* **2013**, *5*, 9640–9644.

[5] Dimroth, F. et al. *Progress in Photovoltaics: Research and Applications* **2014**, *22*, 277–282.

[6] Thompson, B.; Fréchet, J. *Angewandte Chemie International Edition* **2008**, *47*, 58–77.

[7] Wilson, N. R.; Nguyen, P. V.; Seyler, K.; Rivera, P.; Marsden, A. J.; Laker, Z. P. L.; Constantinescu, G. C.; Kandyba, V.; Barinov, A.; Hine, N. D. M.; Xu, X.; Cobden, D. H. *Science Advances* **2017**, *3*, e1601832.

[8] Mann, J. A.; Dichtel, W. R. *The Journal of Physical Chemistry Letters* **2013**, *4*, 2649–2657.

[9] MacLeod, J. M.; Rosei, F. *Small* **2014**, *10*, 1038–1049.

[10] Wei, X.; Tong, W.; Fidler, V.; Zimmt, M. B. *Journal of Colloid and Interface Science* **2012**, *387*, 221–227.

[11] Russell, S. R.; Claridge, S. A. **2016**,

[12] Okawa, Y.; Akai-Kasaya, M.; Kuwahara, Y.; K. Mandal, S.; Aono, M. *Nanoscale* **2012**, *4*, 3013–3028.

[13] Okawa, Y.; Aono, M. *The Journal of Chemical Physics* **2001**, *115*, 2317–2322.

[14] Bang, J. J.; Rupp, K. K.; Russell, S. R.; Choong, S. W.; Claridge, S. A. *Journal of the American Chemical Society* **2016**, *138*, 4448–4457.

[15] Choong, S. W.; Russell, S. R.; Bang, J. J.; Patterson, J. K.; Claridge, S. A. *ACS Applied Materials & Interfaces* **2017**, *9*, 19326–19334.

[16] Hayes, T. R.; Bang, J. J.; Davis, T. C.; Peterson, C. F.; McMillan, D. G.; Claridge, S. A. **2017**,

[17] Davis, T. C.; Bang, J. J.; Brooks, J. T.; McMillan, D. G.; Claridge, S. A. Hierarchically Patterned Noncovalent Functionalization of 2D Materials by Controlled Langmuir–Schaefer Conversion. https://pubs.acs.org/doi/abs/10.1021/acs.langmuir.7b03845, 2018.

[18] Wang, Q. H.; Hersam, M. C. *Nature Chemistry* **2009**, *1*, 206–211.

[19] Love, J. C.; Estroff, L. A.; Kriebel, J. K.; Nuzzo, R. G.; Whitesides, G. M. **2005**,

[20] Pokroy, B.; Aizenberg, J. *CrystEngComm* **2007**, *9*, 1219–1225.

[21] Aizenberg, J.; Black, A. J.; Whitesides, G. M. *Nature* **1999**, *398*, 495–498.

[22] Mezour, M. A.; Voznyy, O.; Sargent, E. H.; Lennox, R. B.; Perepichka, D. F. **2016**,

[23] Pokroy, B.; Chernow, V. F.; Aizenberg, J. *Langmuir* **2009**, *25*, 14002–14006.

[24] Aizenberg, J.; Black, A. J.; Whitesides, G. M. **1998**,

[25] Cao, Y.; Fatemi, V.; Fang, S.; Watanabe, K.; Taniguchi, T.; Kaxiras, E.; Jarillo-Herrero, P. *Nature* **2018**, *556*, 43–50.

[26] Grim, P. C.; De Feyter, S.; Gesquiere, A.; Vanoppen, P.; Rucker, M.; Valiyaveettil, S.; Moessner, G.; Mullen, K.; De Schryver, F. C. **1997**,

[27] Villarreal, T. A.; Russell, S. R.; Bang, J. J.; Patterson, J. K.; Claridge, S. A. **2017**,

[28] Wegner, G. *Die Makromolekulare Chemie* **1972**, *154*, 35–48.

[29] Friesner, R. A.; Banks, J. L.; Murphy, R. B.; Halgren, T. A.; Klicic, J. J.; Mainz, D. T.; Repasky, M. P.; Knoll, E. H.; Shelley, M.; Perry, J. K.; Shaw, D. E.; Francis, P.; Shenkin, P. S. *Journal of Medicinal Chemistry* **2004**, *47*, 1739–1749.

[30] Shivakumar, D.; Williams, J.; Wu, Y.; Damm, W.; Shelley, J.; Sherman, W. *Journal of Chemical Theory and Computation* **2010**, *6*, 1509–1519.

[31] Harder, E. et al. *Journal of Chemical Theory and Computation* **2016**, *12*, 281–296.